

The distribution of forces affects vibrational properties in hard sphere glasses

E. DeGiuli¹, E. Lerner¹, C. Brito², M. Wyart¹

¹*New York University, Center for Soft Matter Research,
4 Washington Place, New York, NY, 10003, USA and*

²*Instituto de Física da UFRGS, 3308-7286 Av. Bento Gonçalves, Porto Alegre, RS, Brasil*

(Dated: July 20, 2022)

We study how the distribution of contact forces, known to behave at small forces as $P(f) \sim f^{\theta_f}$, affects the stability and the vibrational properties of hard sphere glasses. As the jamming transition is approached we predict (i) the density of states $D(\omega) \sim \omega^a$ where $a = (\theta_f - 1)/(3 + \theta_f)$ and ω is the frequency, (ii) the shear modulus $\mu \sim (\phi_c - \phi)^{-b}$ where $b = (4 + 2\theta_f)/(3 + \theta_f)$ and ϕ is the packing fraction and (iii) the mean square displacement $\langle \delta R^2 \rangle \sim (\phi_c - \phi)^\kappa$, where $\kappa = 2 - 2/(3 + \theta_f)$. We test numerically (i) and provide data supporting that $\theta_f \approx 0.17$ independently of the system preparation in two and three dimensions, leading to $\kappa \approx 1.37$, $a \approx -0.26$, and $b \approx 1.37$. Relation (iii) was previously unnoticed but appears to be satisfied in a recent replica calculation in infinite dimension, supporting that this approach captures some vibrational effects very precisely. However, our analysis supports that small and infinite dimension behave differently.

PACS numbers: 63.50.-x, 63.50.Lm, 45.70.-n, 47.57.E-

The emergence of rigidity near the glass transition is a fundamental and highly debated topic in condensed matter, and is perhaps most surprising in hard sphere glasses where rigidity is purely entropic in nature. The rapid growth of relaxation time around a packing fraction $\phi \approx 0.58$ suggests that meta-stable states have appeared in the free energy landscape, and that activation above barriers is required for the system to flow [1]. This scenario is presumably what Mode Coupling Theory captures [2], can be rationalized via density functional theory [3] and via the replica method [4]. However it is only recently that a real-space description of rigidity in hard sphere glasses has emerged [5, 6], based on two results. First, in elastic networks and athermal packings of soft spheres near the unjamming transition [7–9], mechanical stability is controlled by the mean coordination z (as already discussed by Maxwell [10]) and the applied compressive strain e [9]. Second, within a meta-stable state the vibrational free energy of hard spheres can be approximated as a sum of local interaction terms between pairs of colliding particles, which are said to be “in contact”. The interaction follows $V(h) = -k_B T \log h$ where h is the time-averaged distance between two adjacent particles [5, 6]. This results maps the coarse-grained free-energy of hard spheres to the energy of elastic networks at zero temperature. It yields a constraint on the microscopic structure of hard sphere glasses, which in practice appears to lie very close to saturation [5, 6, 11]. Such *marginal stability* implies the abundance of very soft elastic modes, as observed [5, 6, 11–15], and fixes the scaling behavior of elasticity as jamming is approached [6]. In particular the particle mean-square displacement was predicted to follow $\langle \delta R^2 \rangle \sim (\phi_c - \phi)^\kappa$ with $\kappa = 1.5$ instead of the naive $\kappa = 2$.

Very recently a replica calculation [16] predicted $\kappa = 1.41574$ in infinite dimension, at odds with the prediction of [5, 6]. At ϕ_c it also predicted for the force distribution

$P(f) \sim f^{\theta_f}$ with $\theta_f = 0.42311$ and for the gap distribution $g(h) \sim h^{-\gamma}$ with $\gamma = 0.41269$. Some of these latter results are consistent, and some differ, from an earlier analysis based on the stability toward non-linear excitations in packings [17, 18]. Here we propose a resolution of these issues: the heterogeneity in the contact strength, not important for harmonic or Hertzian soft particles, is important for hard spheres and was not included in [5, 6], and leads to the scaling relation $\kappa = 2 - 2/(3 + \theta_f)$ consistent with the result of [16]. We compute the associated modification in the scaling of elastic properties as $\phi \rightarrow \phi_c$. Furthermore, we argue that some key properties of packing differ in finite and infinite dimensions, leading to a description of packings in terms of four exponents related by three scaling relations. In the proposed description, where $\kappa \approx 1.37$, the value of one exponent γ is missing, and appears to be quite well captured by the replica approach.

Model: We consider an elastic network of N points of mass m , connected by N_c springs, of coordination $z = 2N_c/N$, in spatial dimension d . The quadratic expansion of the elastic energy for an imposed displacement field $|\delta R\rangle$ follows [19, 20]:

$$\delta E \equiv \frac{1}{2} \langle \delta R | \mathcal{M} | \delta R \rangle = \frac{1}{2} \sum_{\langle ij \rangle} k_{ij} [(\delta \vec{R}_i - \delta \vec{R}_j) \cdot \vec{n}_{ij}]^2 - \frac{f_{ij}}{2r_{ij}} [(\delta \vec{R}_i - \delta \vec{R}_j) \cdot \vec{n}_{ij}^\perp]^2 \quad (1)$$

where $\langle ij \rangle$ labels the spring going from particle i to j , r_{ij} , k_{ij} , f_{ij} and \vec{n}_{ij} are the spring length, stiffness, force (chosen positive for a repulsive interaction) and direction, and where $\vec{X} \cdot \vec{n}_{ij}^\perp$ indicates the projection of the vector \vec{X} on the plane orthogonal to \vec{n}_{ij} . We assume that the r_{ij} are narrowly distributed about their mean $\langle r_{ij} \rangle = \sigma$ which defines our unit length, and introduce $k_0 \equiv \langle k_{ij} \rangle$ and $\omega_c = \sqrt{k_0/m}$. Eq.(1) defines the stiffness matrix \mathcal{M} ,

which is positive definite in a stable configuration. The eigenvalues of \mathcal{M} are $\lambda = m\omega^2$, where the ω 's are the frequencies of vibrational modes, of density $D(\omega)$.

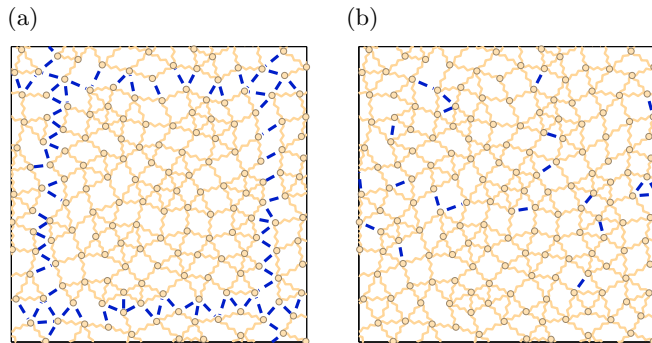


FIG. 1. Illustrative diagram of cutting argument, showing cut bonds in blue (thick lines). (a) Bonds are cut around blocks of size $L \times L$, a useful procedure when $\alpha > 0$; (b) When $\alpha < 0$, the variational argument is improved by cutting instead the fraction q of weakest bonds.

Variational argument: First we consider the springs at rest, $f_{ij} = 0$. Let $\delta z \equiv z - z_c$ with $z_c = 2d$. As pointed out by Maxwell, if $Nd > N_c$ (or equivalently $\delta z < 0$) it is clear that Eq.(1) will have at least $Nd - N_c$ displacement fields with no restoring force ($\delta E = 0$), the so-called floppy modes. We assume that the shape of the stiffness distribution $\mathbb{P}(k)$ is independent of z , and wish to compute the scaling properties of $D(\omega)$ as $\delta z \rightarrow 0^+$. Our strategy is to build trial modes, which are orthonormal displacement fields with small energy. Using the fact that \mathcal{M} is positive definite then allows one to bound from below the number of eigenvalues below some threshold, leading to a lower bound on $D(\omega)$. This strategy was used in [9, 21], where trial modes were constructed from the floppy modes that appear by cutting the system into some compact blobs of size L , as shown in Fig. 1a. The density of floppy modes is simply the fraction of contacts cut, $q \sim 1/L$. These modes can be distorted to lead to trial modes of frequency $\omega(L) \sim \omega_c/L \sim \omega_c q$ in the original, uncut system [21]. Since the density of states is the density of modes per frequency, one gets $D(\omega) \gtrsim q(\omega)/\omega \sim \omega^0/\omega_c$, implying that the vibrational spectrum does not vanish at zero frequency near the Maxwell bound. If $\delta z > 0$, this argument leads to a cut-off frequency $\omega^* \sim \omega_c \delta z$, such that $D(\omega) \gtrsim 1/\omega_c$ above ω^* , as observed numerically [7–9, 22, 23].

We now show that if the distribution of stiffnesses is broad enough, then the above bound is not saturated. In this case, we can improve the variational argument by creating a different set of trial modes, as shown in Fig. 1b. We let $\mathbb{P}(k) \sim k^\alpha/k_0^{\alpha+1}$ at low stiffnesses, where $\alpha > -1$. Let $\delta z \equiv z - z_c > 0$. We cut the fraction q of weakest links, whose characteristic stiffness k_c follows $\int_0^{k_c} \mathbb{P}(k) dk = q$, leading to $k_c \sim k_0 q^{1/(1+\alpha)}$. Then a

fraction $q - \frac{1}{2}\delta z$ of modes in the system are floppy. In the original system, these modes stretch or compress the fraction q of weak springs of characteristic stiffness k_c , and thus have a finite energy of order $E \propto qk_c$, leading to a characteristic frequency:

$$\omega(q) \propto \sqrt{E/m} \sim \omega_c q^{(2+\alpha)/(2+2\alpha)} \quad (2)$$

The variational inequality implies $D(\omega) \gtrsim (q - \frac{1}{2}\delta z)/\omega$. This argument can be applied with any $q \ll 1$ such that $q > \frac{1}{2}\delta z$, implying that $\omega \gtrsim \omega_c \delta z^{(2+\alpha)/(2+2\alpha)}$. It is convenient to let $q = r\delta z$ with $r > \frac{1}{2}$. Then

$$D(\omega) \gtrsim \frac{(1 - 1/(2r))}{\omega_c} \left(\frac{\omega}{\omega_c} \right)^{\alpha/(2+\alpha)} \quad (3)$$

These are our central results: at the Maxwell threshold ($z = z_c$), when weak interactions are abundant ($\alpha < 0$), the density of states must diverge at zero frequency, with a non-trivial exponent. When the coordination is larger ($z > z_c$), the scaling for $D(\omega)$, Eq. (3), holds above the characteristic frequency:

$$\omega^* \sim \omega_c \delta z^{(2+\alpha)/(2+2\alpha)}. \quad (4)$$

For $\alpha > 0$ the previous argument of [21] applies. Note that in all cases we consider $q \ll 1$ so that $\omega \ll \omega_c$. Assuming harmonic dynamics and Eq.(3), one obtains a bound for the particles mean-square displacement $\langle \delta R^2 \rangle$:

$$\frac{k_0 \langle \delta R^2 \rangle}{k_B T} = \omega_c^2 \int \frac{D(\omega)}{\omega^2} d\omega > \omega_c^2 \int_{\omega > \omega^*} \frac{D(\omega)}{\omega^2} d\omega \gtrsim \left(\frac{\omega^*}{\omega_c} \right)^{\frac{-2}{2+\alpha}} \quad (5)$$

To estimate the shear modulus, we cut a fraction $q = \delta z$ of the weakest links, so that the system is now floppy with a density of floppy modes $\frac{1}{2}\delta z$, and no elasticity. It can be shown using the result above for identical springs that under an applied shear of strain ϵ , the relative displacement of particles (of order of the non-affine displacement) is of order $\epsilon/\sqrt{\delta z}$ [24–26]. Including the weak springs, one gets $\delta E \sim qk_c(q)(\epsilon/\sqrt{\delta z})^2$, leading to a shear modulus:

$$\mu \sim k_c \sim k_0 \delta z^{1/(1+\alpha)} \quad (6)$$

Role of pre-stress: the presence of a compressive force in the bonds reduces the modes' frequency, as implied by Eq.(1), and can lead to an elastic instability. It was argued and checked numerically in [9] that the strongly scattered modes that appear above ω^* have large relative displacements, of order of the displacement itself: $[(\delta \vec{R}_i - \delta \vec{R}_j) \cdot \vec{n}_{ij}^\perp] \sim \|\delta \vec{R}_i\|$. Following Eq.(1) this implies that some soft modes will be shifted to a frequency ω_0 satisfying $2\delta E \equiv m\omega_0^2 = m\omega^{*2} - Af$ where f is the characteristic compressive force and A a numerical constant. Stability requires $\omega_0 > 0$, implying $\omega^* > \sqrt{Af/m}$ and $\delta z \gtrsim e^{(1+\alpha)/(2+\alpha)}$ using Eq.(4) and defining the contact strain $e \equiv f/k_0$. This extends the previous result

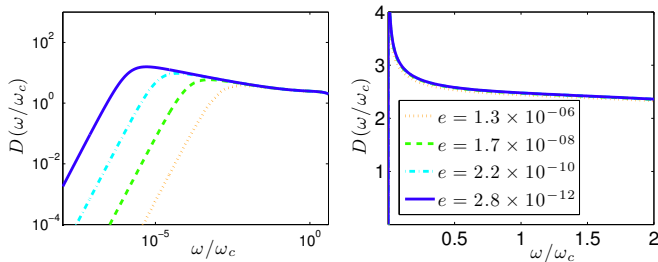


FIG. 2. Effective medium prediction for the density of states $D(\omega)$ for a marginally-stable hard-disk glass with $\theta_f = 0.17$, at indicated values of $e = \phi_c - \phi$, in (left) log-log axes, and (right) linear axes. The peak appears at the frequency scale $\omega^* \sim \omega_c \sqrt{e}$.

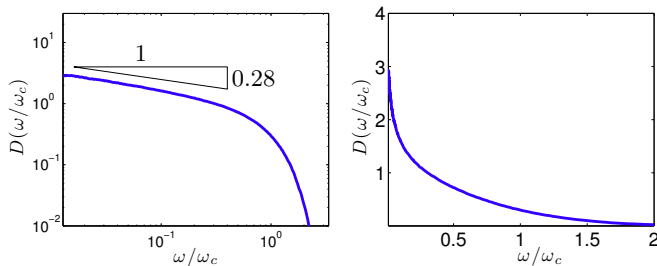


FIG. 3. Numerical density of states $D(\omega)$ for a hard-sphere glass in $d = 2$, at pressure $p = 10^{12}$, in (left) log-log axes, and (right) linear axes. The triangle has the predicted slope -0.28 , assuming $\theta_f = 0.17$, as discussed in the main text. The characteristic frequency ω^* is expected to be $\sim 10^{-6}\omega_c$, outside the accessible numerical range at this pressure.

$\delta z \gtrsim \sqrt{e}$ [9] to the case $\alpha < 0$. In packings of particles, $e \propto |\phi - \phi_c|$ and the latter bound was argued to be saturated, based on dynamical considerations [5, 6, 9].

Hard spheres: In a hard sphere glass, $f_{ij} \sim k_B T / h_{ij}$ where h_{ij} is the mean (time-averaged) gap between two neighboring hard spheres i and j [6], and the stiffness is $k_{ij} = k_B T / h_{ij}^2$, of characteristic amplitude $k_0 \propto k_B T (\phi_c - \phi)^{-2}$. If $\mathbb{P}(f) \sim f^{\theta_f}$, then $\mathbb{P}(k) \sim k^\alpha$ where $\alpha = (\theta_f - 1)/2 < 0$: there are many contacts that have a very weak stiffness. Stability requires $\omega^* \geq (\phi_c - \phi)^{1/2}$, a result identical to the previous approach [5, 6] neglecting the heterogeneities of stiffnesses. In [6, 11] this bound was observed to be saturated. However the change of shape of $D(\omega)$ alters the prediction for the mean square displacement following Eq.(5). One gets overall:

$$D(\omega) \sim \omega^a \quad \text{with } a = \frac{\theta_f - 1}{3 + \theta_f} \quad (7)$$

$$\langle \delta R^2 \rangle \sim (\phi_c - \phi)^\kappa \quad \text{with } \kappa = 2 - \frac{2}{3 + \theta_f} \quad (8)$$

$$\mu \sim (\phi_c - \phi)^{-b} \quad \text{with } b = \frac{4 + 2\theta_f}{3 + \theta_f} \quad (9)$$

In Supplementary Information (SI), we argue that this

result is not changed if the evolution of $\mathbb{P}(k)$ with packing fraction is taken into account.

Effective Medium: All the above predictions can be derived and extended with effective medium theory (EMT), a mean-field approximation that treats disorder in a self-consistent way [27–33]. EMT has been shown to give quantitatively correct values for scaling exponents related to the vibrational spectrum and heat transport properties of frictionless packings [30, 32]. In EMT, a random elastic network, such as depicted in Figure 1, is modeled by a regular lattice with effective frequency-dependent spring constants. Here we follow the EMT developed in [32] which includes the effect of pre-stress. In [32] the randomness in the interaction between two nodes was limited to the presence or absence of a spring; when a spring was present, its stiffness was always identical. Here we relax this assumption and allow a full distribution of stiffnesses, behaving as $\mathbb{P}(k) \sim k^\alpha$ for small k , and allow a distribution of contact forces, $\mathbb{P}(f) \sim f^{\theta_f}$ at small f . Details of the EMT are presented in the SI.

In addition to confirming the scaling results presented above, EMT gives the form of the complex shear modulus and density of states when δz is small, and can be used to extract other vibrational and heat transport properties. In general, two frequency scales are predicted, as in the variational argument: ω^* and $\omega_0 = \omega^* \sqrt{1 - e/e_c}$, where $e_c \sim \delta z^{(2+\alpha)/(1+\alpha)}$ is the contact strain at elastic instability [32]. For a marginally stable material, $e \approx e_c$ and therefore $\omega_0/\omega^* \ll 1$. Above ω^* , EMT predicts $D(\omega/\omega_c) \sim (\omega/\omega_c)^{\alpha/(2+\alpha)}$, in agreement with Eq. (3), with a logarithmic correction in $d = 2$. Between ω_0 and ω^* , EMT predicts $D(\omega/\omega_c) \sim (\omega/\omega_c)^{1+2/(\alpha+2)} (\omega^*/\omega_c)^{-4/(\alpha+2)}$. Numerical solution of the leading-order EMT equation for hard spheres at $e = e_c$ in $d = 2$ gives the result shown in Figure 2, where we have taken $\theta_f = 0.17$. EMT also predicts the behavior of the shear modulus. We confirm the scaling (6), and in addition find the dependence on e/e_c . At fixed δz , we find that μ drops by a finite factor $(\alpha + 2)^{1/(\alpha+1)}$ at elastic instability, relative to its unstressed value.

Comparison with numerics: To confirm the novel prediction that $D(\omega)$ is not flat but scales with frequency as jamming is approached from the hard sphere side, we perform numerical simulations of a hard-sphere glass in $d = 2$, at pressure $p = 10^{12} k_B T$ and volume fraction $\phi \approx 0.83$ (details are in the Supplementary Information). The density of states $D(\omega)$ can be computed by identifying a contact network via time averaging as done in [5, 6]. Our result for the largest pressure is shown in Fig. 3, confirming the non trivial dependence of $D(\omega)$ with frequency predicted in (3). This prediction could be tested in colloidal systems using static pair correlation to extract \mathcal{M} and $D(\omega)$ [11–15].

Comparison with the replica approach in $d = \infty$: A very recent replica computation in $d = \infty$ claims to compute exponents with five digit precision [16, 34–36], and

gets $\gamma = 0.41269$, $\kappa = 1.41574$ and $\theta_f = 0.42311$. These results are consistent with our newly derived Eq.(8), which appears to be exactly satisfied.

However, the numerical value we found previously [18, 37] for $\theta_f \approx 0.17$ in two and three dimensions differs from the replica computation at $d = \infty$. It was argued based on numerics [38] that exponents weakly depend on spatial dimensions up to $d = 10$, leading to the suggestion that dimension does not play a role. The same work also reported that θ_f depends somewhat on system preparation. To check that our value of θ_f is not due to the specific methods we used (in [37] results were obtained in two dimensions by shear-jamming hard disks, while in [18] hard spheres were compressed in an over-damped medium), we repeat the measurement of force distribution by decompressing soft spheres as done in [38], but with much higher statistics for the dimension considered. Figure 4 shows $\mathbb{P}(f)$ in 3 dimensions, and again we find $\theta_f = 0.17 \pm 0.02$ (details appear in the Supplementary Information). Our results therefore support that system preparation does not affect the exponent θ_f [39], and that its value is indeed about 0.17.

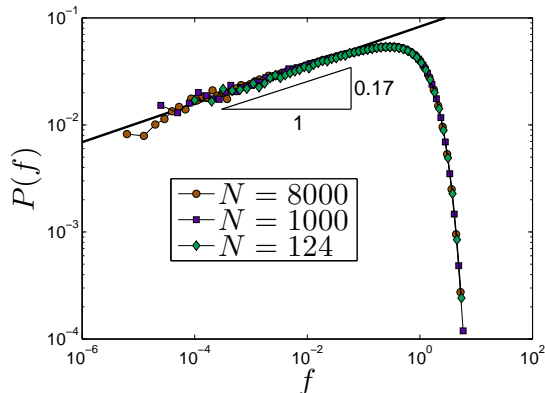


FIG. 4. Probability distribution of forces $\mathbb{P}(f)$ for isostatic packings of soft spheres at indicated system sizes, showing the small-force exponent $\theta_f = 0.17$.

We propose the following explanation for the distinction between small and infinite dimension. In addition to the soft modes discussed above, two distinct nonlinear excitations characterizing jammed packings at ϕ_c have been identified [17, 18], each corresponding to opening a contact at low force. If the contact force is very small, triggering these excitations can lead to the rewiring of the contact network. In some cases, the resulting motion of the particles is mostly local. The density of these *local excitations* as a function of contact forces f follows f^θ . Particle displacements can also be extended; the density of these *extended excitations* follows $f^{\theta'}$. In two and three dimensions it was observed that at low-forces most contacts are associated to localized excitations ($\theta < \theta'$), and the distribution of forces thus follows $\mathbb{P}(f) \sim f^{\theta_f}$ with $\theta_f = \theta$. Stability of the system to extensive avalanches

of rewiring was shown to imply [17, 18]

$$\gamma \geq \frac{1 - \theta}{2} \quad (10)$$

$$\gamma \geq \frac{1}{2 + \theta'} \quad (11)$$

In [18] it was argued that nonlinear excitations in packings are marginally stable with $\gamma \approx 0.4$, $\theta \approx 0.17$ and $\theta' \approx 0.44$. Equations (8) with $\theta_f = \theta$, (10), and (11) lead to a description of jammed packings and glasses in low dimensions based on 4 exponents, with three scaling relations between them. We have in particular $\kappa = 2 - 1/(2 - \gamma)$, and using $\gamma = 0.41$ (the numerical estimate that agrees well with the $d = \infty$ replica calculation), we get the prediction $\kappa \approx 1.37$.

This description is thus inconsistent with the $d = \infty$ result for the values of κ and θ_f . However, if it is assumed that localized excitations do not exist for $d = \infty$, one is left with 3 exponents constrained by two scaling relations: Eq.(11) (where $\theta_f = \theta'$), and Eq.(8). The scaling description we propose based on the marginality of real space excitations (both linear and non-linear) is thus fully consistent with the replica calculation, as these two scaling relations are satisfied. The fact that localized excitations appear to be absent in large dimension seems plausible, as their existence depends on the presence of local arrangements of particles that are very soft, which may become unlikely when each particle shares many contacts. This situation may be similar to the behavior of ‘rattlers’, particles which are trapped in a packing but do not contribute to mechanical stability. The fraction of rattlers is observed to decay *exponentially* with d [38], so that in large dimension, it is extremely rare to find a gap that is large enough to hold a particle. The same exponential decay may occur for localized excitations.

Conclusion: We have shown that the stability of hard spheres glasses is affected by heterogeneity in contact strengths. If the glass is marginally stable, the mean square displacement must diverge with an exponent $\kappa = 2 - 2/(3 + \theta_f) \approx 1.37$ at jamming, and the density of states follows $D(\omega) \sim \omega^{(\theta_f - 1)/(3 + \theta_f)}$, an experimentally testable result in good agreement with our numerics. Overall, our approach leads to a description of jamming in finite dimensions based on the marginal stability of two distinct types of excitations. It remains to be seen if the cause of marginal stability in finite dimension is of dynamical [6, 9] or entropic origin [16], and if plastic flow under shear and thermally activated process near the glass transition can be expressed in terms of the relaxation of these excitations.

Acknowledgments: We thank the authors of [16] for sharing their preprint and for discussions, and Jie Lin, Le Yan, Gustavo Düring and Marija Vucelja for discussions. MW acknowledges support from NSF CBET Grant 1236378, NSF DMR Grant 1105387, and MRSEC Program of the NSF DMR-0820341 for partial funding.

SUPPLEMENTARY INFORMATION

In this Supplementary Information, we provide (A) details of the effective medium theory discussed in the main text, (B) information on the hard-sphere numerical simulations, (C) information on the soft-sphere numerical simulations, and (D) evidence that the change in gap distribution at finite δz does not affect our results.

A. EFFECTIVE MEDIUM THEORY

Our effective medium theory (EMT) is an extension of [32]. The difference in the present work is to allow the bond stiffnesses and contact forces to follow nontrivial distributions $\mathbb{P}(k)$ and $\mathbb{P}(f)$. For the latter, we consider

$$\mathbb{P}(f) = C_f f^\theta e^{-f/\bar{f}}, \quad (\text{A.1})$$

with $0 \leq \theta < 1$ and contact force law

$$f = k_1 |h|^x, \quad (\text{A.2})$$

where h is the gap at a contact ($h < 0$ for overlap). We are interested in the cases $-1 \leq x < 0$ and $x > 1$. We assume particle diameter $\sigma = 1$ so that k_1 has units of stiffness. The contact stiffness is $k = df/dh \propto |h|^{x-1}$. This implies

$$\mathbb{P}(k) = C_k k^\alpha e^{-(k/\bar{k})^{x/(x-1)}} \quad (\text{A.3})$$

with $\alpha = (1 + x\theta)/(x - 1)$. We have $\alpha > 0$ when $x > 1$ and $\alpha < 0$ when $x < 0$. The contact strain e is defined by $e \equiv \langle f \rangle / \langle k \rangle$. We take units with $\bar{k} = 1$.

As in previous work, we model a random elastic network of coordination z by diluting a regular lattice of coordination z_0 down to z . The stiffness in contact α , k_α , and the force in the contact, f_α are random variables distributed according to

$$\mathbb{P}_{EMT}(k_\alpha) = (1 - P)\delta(k_\alpha) + P \mathbb{P}(k_\alpha) \quad (\text{A.4})$$

$$\mathbb{P}_{EMT}(f_\alpha) = (1 - P)\delta(f_\alpha) + P \mathbb{P}(f_\alpha) \quad (\text{A.5})$$

where $P = z/z_0$ to model random dilution of the lattice.

In EMT, the elastic behavior of a random material, such as our randomly diluted lattice, is modelled by a regular lattice with effective frequency-dependent stiffnesses; as in [32] we will have a longitudinal stiffness, k^\parallel , and a transverse stiffness $-ek^\perp$. Writing $\bar{\cdot}$ for disorder average, the EMT equations are, from [32],

$$0 = \frac{k^\parallel - k_\alpha}{1 - (k^\parallel - k_\alpha)G^\parallel} = \frac{ek^\perp - f_\alpha}{1 + (ek^\perp - f_\alpha)G^\perp}, \quad (\text{A.6})$$

where G^\parallel and G^\perp are related to the Green's function $(\omega) = (\mathcal{M} - m\omega^2)^{-1}$ by

$$G^\parallel = 2n_\alpha \cdot \langle \alpha | G | \alpha \rangle \cdot n_\alpha \quad (\text{A.7})$$

$$G^\perp = 2\text{tr}(\langle \alpha | G | \alpha \rangle) - G^\parallel, \quad (\text{A.8})$$

with $\langle \alpha | \equiv \langle i | - \langle j |$. In the present case this leads to

$$0 = \frac{(1 - P)k^\parallel}{1 - k^\parallel G^\parallel} + PC_k \left[-\frac{1}{C_k G^\parallel} + \frac{1}{G^\parallel} \frac{\beta}{G^\parallel} \int_0^\infty df \frac{f^\theta e^{-f}}{c + f^\beta} \right] \quad (\text{A.9})$$

$$0 = \frac{(1 - P)ek^\perp}{1 + ek^\perp G^\perp} + PC_f \left[\frac{1}{C_f G^\perp} - \frac{\bar{f}^\theta}{G^{\perp 2}} \int_0^\infty df \frac{f^\theta e^{-f}}{c_2 - f} \right], \quad (\text{A.10})$$

with $\beta = 1 - 1/x$, $c = (1 - k^\parallel G^\parallel)/G^\parallel$, and $c_2 = (1 + ek^\perp G^\perp)/(\bar{f} G^\perp)$. These equations need to be supplemented with an equation for G . As in [32], we consider a simplified continuum-like Green's function with a single elastic modulus, and whose isotropy has been restored. This is

$$G(r, \omega) = \frac{z_0 \hat{\delta}}{d} \int_{BZ} \frac{d^d q}{(2\pi)^d} \frac{e^{iq \cdot r}}{(k^\parallel - ek^\perp)q^2 - m\omega^2}, \quad (\text{A.11})$$

where $BZ = \{q : |q| < \Lambda\}$ is an approximate first Brillouin zone, and $\hat{\delta}$ is the identity tensor. Isotropy of G implies an identity

$$G^\parallel = G^\perp = \frac{2d}{z_0} \frac{1}{k^\parallel - ek^\perp} \left(1 + \frac{m\omega^2}{d} \text{tr}(G(0, \omega)) \right) \quad (\text{A.12})$$

which closes the model. We solve equations (A.9), (A.10), (A.11), and (A.12) in the limit $e \ll 1$ and $\delta z = z - z_c \ll 1$. Based on previous results [32], we expect $|c| \ll 1$ and $|c_2| \gg 1$ (which can be checked *a posteriori*), which allows an expansion

$$\int_0^\infty df \frac{f^\theta e^{-f}}{c + f^\beta} = \begin{cases} -\frac{c^\alpha \pi}{\beta \sin(\pi\alpha)} + \dots & \text{if } -1 < \alpha < 0 \\ \Gamma_{\alpha\beta} + \dots & \text{if } \alpha > 0, \end{cases} \quad (\text{A.13})$$

with $\Gamma_t = \int_0^\infty x^{t-1} e^{-x} dx$. From this result it can be deduced that for $\alpha > 0$, the previous results of [32] are obtained, up to prefactors which depend on θ and x . Henceforth, we consider only $\alpha < 0$, corresponding to an abundance of weak springs, as discussed in the main text. The other integral is found similarly

$$\int_0^\infty df \frac{f^\theta e^{-f}}{c_2 - f} = \frac{\Gamma_{\theta+1}}{c_2} + \frac{\Gamma_{\theta+2}}{c_2^2} + \mathcal{O}(1/c_2^3) \quad (\text{A.14})$$

The leading order EMT equations are then

$$0 = k^\parallel G^\parallel - P + \frac{(1 - k^\parallel G^\parallel)^{\alpha+1} P}{G^{\parallel \alpha+1} \Gamma_{\theta+1}} \frac{\pi}{\beta \sin(\pi|\alpha|)} \quad (\text{A.15})$$

$$0 = ek^\perp G^\perp - \frac{P \bar{f} G^\perp (\theta + 1)}{1 + ek^\perp G^\perp} \quad (\text{A.16})$$

Assuming $\omega \ll \sqrt{k^\parallel/m}$, it can be checked that

$$\frac{1}{d} \text{tr}[G(0, \omega)] = \frac{A_1}{k^\parallel - ek^\perp} + \dots \quad (\text{A.17})$$

with

$$A_1 = \frac{z_0}{d} \frac{2\pi^{d/2}}{\Gamma_{d/2}(2\pi)^d} \begin{cases} \frac{\Lambda^{d-2}}{d-2} & \text{if } d \geq 3 \\ \frac{1}{2} \log(1/\delta z) & \text{if } d = 2 \end{cases} \quad (\text{A.18})$$

The above equations can be solved for $\delta z \ll 1$ following the procedure in [32]: we let

$$k^{\parallel} \sim \delta z^{\xi}, \quad ek^{\perp} \sim \delta z^{\eta}, \quad e = e_c e' \quad (\text{A.19})$$

$$e_c \sim \delta z^{\chi}, \quad \omega \sim \delta z^{\zeta} \quad (\text{A.20})$$

and balance terms in the above equations. Note that e and δz are independent parameters: in an elastic network they can be controlled independently. Here e_c is the critical contact strain at elastic instability [32]. One finds

$$\xi = 1/(\alpha + 1), \quad (\text{A.21})$$

$$\chi = \eta = 2\zeta = 1 + \xi = \frac{\alpha + 2}{\alpha + 1} \quad (\text{A.22})$$

reproducing the scalings in the main text. To leading order, the transverse stiffness is

$$k^{\perp} = \frac{2d(\theta + 1)\Gamma_{\theta+2-1/x}}{z_0 \Gamma_{\theta+2}} \quad (\text{A.23})$$

while the leading order equation for k^{\parallel} is

$$0 = 2dA_1\omega^2 - k^{\parallel}\delta z + ek^{\perp}z_c + k^{\parallel\alpha+2}c_3 \quad (\text{A.24})$$

with $c_3 = \pi z_0(1 - 2d/z_0)^{\alpha+1}(z_0/(2d))^{\alpha}/(\Gamma_{\theta+1} \sin(\pi|\alpha|))$. This is a transcendental equation for k^{\parallel} that does not have an analytic solution. However, we can determine some of its key properties.

We expect an onset frequency ω_0 where the density of states $D(\omega)$ grows from 0. This requires that at ω_0 , $|dk^{\parallel}/d\omega| = \infty$, giving

$$\omega_0 = \omega^* \sqrt{1 - e/e_c} \quad (\text{A.25})$$

with $\omega^* = \delta z^{\zeta} \sqrt{c_4/(z_c A_1)}$, $e_c = \delta z^{2\zeta} c_4/(2dk^{\perp})$, and $c_4 = (c_3(\alpha + 2))^{-1/(\alpha+1)}/\eta$. The onset frequency ω_0 vanishes at elastic instability $e = e_c$.

Below ω_0 , $k^{\parallel} \approx k_0^{\parallel} = k^{\parallel}(\omega_0) = (\delta z/(c_3(\alpha + 2)))^{1/(\alpha+1)}$. For $\omega \gg \omega_0$, we find instead $k^{\parallel} \approx \omega^{2/(\alpha+2)}(-2dA_1/c_3)^{1/(\alpha+2)}$. Combining these gives the approximate solution

$$k^{\parallel} \approx k_0^{\parallel} + \omega^{2/(\alpha+2)}(-2dA_1/c_3)^{1/(\alpha+2)}. \quad (\text{A.26})$$

The density of states is determined by

$$D(\omega) = \frac{z_0}{\pi\omega} \text{Im}[(k^{\parallel} - ek^{\perp})G^{\parallel}] \quad (\text{A.27})$$

$$= \frac{2dA_1}{\pi} \omega \text{Im}[1/(k^{\parallel} - ek^{\perp})] + \dots \quad (\text{A.28})$$

which readily gives

$$D(\omega) \sim \begin{cases} 0 & \text{if } \omega < \omega_0 \\ \omega^{1+2/(\alpha+2)}\delta z^{-2/(\alpha+1)} & \text{if } \omega_0 < \omega < \omega_* \\ \omega^{1-2/(\alpha+2)} & \text{if } \omega > \omega_* \end{cases} \quad (\text{A.29})$$

For a marginally stable material, $e/e_c \ll 1$ so that $\omega_0 = 0$. Hard spheres correspond to $x = -1$ and $k_1 = k_B T \sim 1$ in our units. The predicted behavior in this case is shown in Figs. 1 and 2 in the main text, for $d = 2$, corresponding to hard disks. Note that for hard disks, assuming $\theta \approx 0.17$, we have $\alpha = -0.42$, $1 + 2/(\alpha + 2) = 2.26$, and $1 - 2/(\alpha + 2) = -0.26$.

Finally, the shear modulus is $\mu = k^{\parallel}(\omega = 0)$. When $e = 0$, we find

$$\mu(e = 0) = \left(\frac{\delta z}{c_3}\right)^{1/(\alpha+1)}, \quad (\text{A.30})$$

while when $e = e_c$, $\mu(e = e_c) = k_0^{\parallel}$, so that μ is smaller by a factor of

$$\frac{\mu(e = 0)}{\mu(e = e_c)} = (\alpha + 2)^{1/(\alpha+1)} \quad (\text{A.31})$$

at instability. Note that when $\alpha = 0$ we recover the factor 2 found in earlier theory [32, 40].

B. HARD-SPHERE NUMERICAL SIMULATIONS

We simulate hard disks using an event-driven molecular dynamics code [41], in which particles are in free flight until they collide elastically. The system is 50:50 bidisperse, with size ratio 1.4. We take units with small diameter $\sigma_1 = 1$, mass $m = 1$ (the same for both species), and $k_B T = 1$, so that time is measured in units of $\sqrt{m\sigma_1/(k_B T)}$. To generate very large packings, we start with random configurations at very low density and use the Lubachevsky-Stillinger algorithm, in which particles are inflated [42]. The particle inflation rate Γ varies with pressure p as $\Gamma = 10^{-3}$ up to $p = 10^2$ and $\Gamma = 10^{-5}$ up to $p = 10^{12}$. At $p = 10^{12}$ the packing fraction is distributed around $\phi_c \approx 0.83$. This protocol generates isostatic packings at ϕ_c , as was explicitly checked in all the packings used. To obtain configurations at $\phi < \phi_c$, particles are then deflated by a relative amount ϵ , and assigned random velocities. Note that $\frac{1}{2}Nzk_B T = p(V - V_c) \approx p(\phi_c - \phi)N3\pi/(2\phi_c^2)$ so that $p(\phi_c - \phi) \approx 0.29k_B T$.

To measure the vibrational spectrum of hard disks, it is necessary to define a contact force network within an interval of time Δt [5, 6]. Two particles are said to be in contact if they collide with each other during Δt . In this same interval, we define h_{ij} as the average gap between

two particles and the contact force f_{ij} as the average momentum they exchange per unit of time. We can then define an effective potential $V_{eff} = -k_B T \log h_{ij}$ [5, 6], which allows a computation of the dynamical matrix \mathcal{M} . In this work we choose $\Delta t = 1000N$ collisions and $N = 4096$ particles. For larger Δt , the vibrational spectrum does not change in the frequency range shown.

C. SOFT-SPHERE NUMERICAL SIMULATIONS

We prepare three-dimensional isostatic packings of bi-disperse soft-spheres, of which half are large and half are small, with the ratio of their respective radii set to 1.4. With ρ_i denoting the radius of the i^{th} particle, and r_{ij} denoting the pairwise distance between the centers of particles i and j , the pairwise potential reads $\phi(r_{ij}) = \frac{k}{2}(r_{ij} - (\rho_i + \rho_j))^2$, where k is the stiffness. We generate isostatic packings by performing a fast quench of a random configuration using the FIRE algorithm [43] and applying compressive or expansive strains followed by additional quenches to obtain the target coordination of $z_c = 6$. We choose the stopping condition of the quenches to be $\|\vec{F}^{\text{max}}\|/\langle f \rangle < 10^{-8}$, where $\|\vec{F}^{\text{max}}\|$ is the magnitude of the maximum (over all particles in a packing) of the net force, and $\langle f \rangle$ is the mean contact force. We note that for our largest systems of $N = 8000$ particles, the isostatic point occurs at dimensionless pressures of the order 10^{-9} or smaller; equilibrating packings mechanically at such pressures requires quad floating point precision numerics.

D. EFFECT OF CHANGE OF STIFFNESS DISTRIBUTION WITH ϕ

In the main text and in the EMT described above, we have assumed that the shape of the distribution of stiffnesses, $\mathbb{P}(k)$, is independent of δz and e . For hard spheres, we have $f = k_B T/h$ and $k = k_B T/h^2$, where h is the average gap between particles, given that they share a contact (in the sense of [6]). The main effect of changing ϕ is to rescale the characteristic stiffness k_0 , which is included in our approach. However as discussed in [38] one expects the rescaled distribution of gaps (and therefore of stiffnesses) to evolve as ϕ departs from ϕ_c at weak forces. Here we argue that this evolution, and the presence of additional contacts at large distance and small force, does not alter our prediction on κ (although it could affect the scaling of δz , a difficult question). For simplicity we shall consider that all particles at distance $h \lesssim 1$ share a contact (a scenario presumably much worse than what occurs in packings where contacts are plausibly not made as soon as $h \gg h_\dagger$ defined below). We let $k_B T = 1$.

The hard-sphere gap distribution $g(h)$ has 2 scaling

regimes (denoted Ib and IIIb in [38]), and an intermediate matching regime (denoted IIb in [38]). In the first scaling regime, corresponding to gaps that become contacts in the limit $p \rightarrow \infty$, we have

$$g(h) \sim p(hp)^{-2-\theta} \quad \text{if } h \sim p^{-1} \quad (\text{D.1})$$

In the second scaling regime, corresponding to gaps that are small, but not zero, as $p \rightarrow \infty$, we have

$$g(h) \sim h^{-\gamma} \quad \text{if } h \sim 1 \quad (\text{D.2})$$

In [38], these forms are shown to match smoothly in an intermediate regime $h \sim p^{-\mu}$ with $\mu = (1+\theta)/(2+\theta-\gamma)$. Here it will be sufficient to eliminate this intermediate regime by joining the two primary distributions at an intermediate gap size $h_\dagger \sim p^{-\mu}$. We also truncate $g(h)$ at microscopic and macroscopic gap sizes $\delta \ll p^{-1}$ and $h_L \sim 1$. We therefore consider

$$g(h) \sim \begin{cases} p(hp)^{-2-\theta} & \text{if } \delta < h < h_\dagger \\ C_2 h^{-\gamma} & \text{if } h_\dagger < h < h_L \end{cases} \quad (\text{D.3})$$

This implies

$$\mathbb{P}(k) = \frac{C_1}{k^{3/2}} \begin{cases} p(p/\sqrt{k})^{-2-\theta} & \text{if } k_\dagger < k < 1/\delta^2 \\ C_2 k^{\gamma/2} & \text{if } k_L < k < k_\dagger \end{cases} \quad (\text{D.4})$$

where $k_L = 1/h_L^2$ and $k_\dagger = 1/h_\dagger^2$. The constants C_1 and C_2 in these expressions are set by requiring that $\mathbb{P}(k)$ is normalized, and the distribution is continuous at h_\dagger . This implies $C_2 = p^{-1-\theta} k_\dagger^{(2+\theta-\alpha)/2}$.

Since $-3/2 + 1 + \theta/2 = \alpha$ and the cutoff $1/\delta^2$ plays the same role as an exponential cutoff (as in the EMT, Eq. (A.3)), this distribution differs from what is considered in the main text by the ultra-weak force regime $k < k_\dagger$. To show that the presence of this regime does not affect our results, we estimate its relative contribution to the energy in a typical mode, R , as

$$R = \frac{\int_{k_L}^{k_\dagger} dk k \mathbb{P}(k)}{\int_{k_\dagger}^{1/\delta^2} dk k \mathbb{P}(k)} \quad (\text{D.5})$$

$$\sim p^{1+2\theta} \delta^{4+2\alpha} \quad (\text{D.6})$$

We can let $\delta \sim p^{-\nu}$ with $\nu \geq 1$, which implies $R \lesssim p^{\theta-2}$. This goes to zero as $p \rightarrow \infty$, so to leading order the ultra-weak springs contain only an infinitesimal fraction of energy, and will not affect our results.

-
- [1] M. Goldstein, *J. Chem. Phys.* **51**, 3728 (1969).
- [2] L. Berthier and G. Biroli, *Reviews of Modern Physics* **83**, 587 (2011).
- [3] Y. Singh, J. Stoessel, and P. Wolynes, *Physical review letters* **54**, 1059 (1985).
- [4] G. Parisi and F. Zamponi, *Reviews of Modern Physics* **82**, 789 (2010).
- [5] C. Brito and M. Wyart, *EPL (Europhysics Letters)* **76**, 149 (2006).
- [6] C. Brito and M. Wyart, *J. Chem. Phys.* **131**, 024504 (2009).
- [7] A. J. Liu, S. R. Nagel, W. van Saarloos, and M. Wyart, "The jamming scenario: an introduction and outlook," in *Dynamical heterogeneities in glasses, colloids, and granular media*, edited by L. Berthier, G. Biroli, J. Bouchaud, L. Cipeletti, and W. van Saarloos (Oxford University Press, Oxford, 2010).
- [8] M. van Hecke, *Journal of Physics: Condensed Matter* **22**, 033101 (2010).
- [9] M. Wyart, *Annales de Phys* **30** (3), 1 (2005).
- [10] J. Maxwell, *Philos. Mag.* **27**, 294 (1864).
- [11] A. Ikeda, L. Berthier, and G. Biroli, *The Journal of Chemical Physics* **138**, 12A507 (2013).
- [12] A. Ghosh, V. K. Chikkadi, P. Schall, J. Kurchan, and D. Bonn, *Physical review letters* **104**, 248305 (2010).
- [13] K. Chen, W. G. Ellenbroek, Z. Zhang, D. T. Chen, P. J. Yunker, S. Henkes, C. Brito, O. Dauchot, W. Van Saarloos, A. J. Liu, *et al.*, *Physical review letters* **105**, 025501 (2010).
- [14] D. Kaya, N. Green, C. Maloney, and M. Islam, *Science* **329**, 656 (2010).
- [15] R. Mari, F. Krzakala, and J. Kurchan, *Phys. Rev. Lett.* **103**, 025701 (2009).
- [16] P. Charbonneau, J. Kurchan, G. Parisi, P. Urbani, and F. Zamponi, *arXiv preprint arXiv:1310.2549* (2013).
- [17] M. Wyart, *Phys. Rev. Lett.* **109**, 125502 (2012).
- [18] E. Lerner, G. Düring, and M. Wyart, *Soft Matter* (2013).
- [19] L. D. Landau and E. Lifshitz, *Theory of Elasticity: Vol. 7 of Course of Theoretical Physics*, Vol. 13 (1960) p. 44.
- [20] S. Alexander, *Physics Reports* **296**, 65 (1998).
- [21] M. Wyart, S. Nagel, and T. Witten, *EPL (Europhysics Letters)* **72**, 486 (2005).
- [22] C. S. O'Hern, L. E. Silbert, A. J. Liu, and S. R. Nagel, *Phys. Rev. E* **68**, 011306 (2003).
- [23] L. E. Silbert, A. J. Liu, and S. R. Nagel, *Phys. Rev. Lett.* **95**, 098301 (2005).
- [24] M. Wyart, H. Liang, A. Kabla, and L. Mahadevan, *Phys. Rev. Lett.* **101**, 215501 (2008).
- [25] W. G. Ellenbroek, Z. Zeravcic, W. van Saarloos, and M. van Hecke, *EPL (Europhysics Letters)* **87**, 34004 (2009).
- [26] W. G. Ellenbroek, E. Somfai, M. van Hecke, and W. van Saarloos, *Phys. Rev. Lett.* **97**, 258001 (2006).
- [27] E. J. Garboczi and M. F. Thorpe, *Phys. Rev. B* **31**, 7276 (1985).
- [28] W. Schirmacher, G. Ruocco, and T. Scopigno, *Phys. Rev. Lett.* **98**, 025501 (2007).
- [29] I. Webman, *PRL* **47**, 1496 (1981).
- [30] M. Wyart, *EPL (Europhysics Letters)* **89**, 64001 (2010).
- [31] X. Mao, N. Xu, and T. C. Lubensky, *Phys. Rev. Lett.* **104**, 085504 (2010).
- [32] E. DeGiuli, A. Laversanne-Finot, G. Düring, E. Lerner, and M. Wyart, *arXiv preprint arXiv:1401.6563* (2014).
- [33] M. Sheinman, C. Broedersz, and F. MacKintosh, *Physical Review E* **85**, 021801 (2012).
- [34] J. Kurchan, G. Parisi, and F. Zamponi, *Journal of Statistical Mechanics: Theory and Experiment* **2012**, P10012 (2012).
- [35] J. Kurchan, G. Parisi, P. Urbani, and F. Zamponi, *The Journal of Physical Chemistry B* **117**, 12979 (2013).
- [36] G. Parisi, *arXiv preprint arXiv:1401.4413* (2014).
- [37] E. Lerner, G. Düring, and M. Wyart, *EPL (Europhysics Letters)* **99**, 58003 (2012).
- [38] P. Charbonneau, E. I. Corwin, G. Parisi, and F. Zamponi, *Physical Review Letters* **109**, 205501 (2012).
- [39] Note that in all cases the systems considered are bidisperse; we find that monodisperse packings in 3 dimensions have a slightly larger exponent $\theta_f \approx 0.21$.
- [40] H. Yoshino, *The Journal of Chemical Physics* **136**, 214108 (2012).
- [41] M. P. Allen and D. J. Tildesley, *Computer simulation of liquids* (Oxford university press, 1989).
- [42] A. Donev, S. Torquato, and F. H. Stillinger, *Phys. Rev. E* **71**, 011105 (2005).
- [43] E. Bitzek, P. Koskinen, F. Gähler, M. Moseler, and P. Gumbsch, *Phys. Rev. Lett.* **97**, 170201 (2006).